Crack-Induced Anisotropy in Crustal Rocks: Predicted Dry and Fluid-Saturated Thomsen's Parameters

Yves Guèguen, Joël Sarout

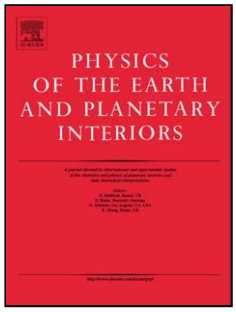

Title: Crack-Induced Anisotropy in Crustal Rocks: Predicted Dry and Fluid-Saturated Thomsen's Parameters

Authors: Yves Guèguen, Joël Sarout

PII: S0031-9201(08)00109-X
DOI: doi:10.1016/j.pepi.2008.05.020
Reference: PEPI 4952

To appear in: *Physics of the Earth and Planetary Interiors*

Received date: 17-9-2007
Revised date: 22-4-2008
Accepted date: 29-5-2008

Please cite this article as: Guèguen, Y., Sarout, J., Crack-Induced Anisotropy in Crustal Rocks: Predicted Dry and Fluid-Saturated Thomsen's Parameters, *Physics of the Earth and Planetary Interiors* (2007), doi:10.1016/j.pepi.2008.05.020

Crack-Induced Anisotropy in Crustal Rocks: Predicted Dry and Fluid-Saturated Thomsen's Parameters

Yves Guéguen* and Joël Sarout

Laboratoire de Géologie
Ecole Normale Supérieure - CNRS UMR 8538
24 rue Lhomond - 75005 - Paris - France

**Corresponding author. E-mail: yves.gueguen@ens.fr. Fax: 33 (0)1 44 32 20 00*

Abstract

In upper crustal conditions, elastic anisotropy of rocks is mainly due to cracks, as long as the anisotropy of the background matrix remains low. Because, in general, rock anisotropy remains weak, in the sense that hexagonal symmetry may be sufficient to handle it, Thomsen suggested that a set of three parameters would be convenient to describe it. Using effective elasticity, we derive Thomsen's parameters for the case of dry and fluid-saturated cracks, in a rock of isotropic background, in terms of crack density parameters and fluid compressibility. These results can be of interest for the interpretation of seismological and seismic data. They provide moreover a way to identify the fluid nature (gas or liquid) and to extract the crack density tensor from elastic wave data. Frequency effects are discussed when fluid is present so that frequency dependence can be accounted for.

Key words: Crustal Rocks; Cracks; Elastic wavespeeds; Seismic anisotropy; Effective medium theory; Rock properties

1 Introduction

At all scales, from local to regional, rocks are heterogeneous. The influence of heterogeneity in rock, as long as it remains moderate, can often be handled by using the ergodic assumption, considering that the medium is statistically homogeneous. That means that a representative volume element (RVE) exists and that any part of the system with a volume much larger than the RVE has identical physical properties. In this case, the medium can be considered as invariant by translation (for any property averaged over a RVE). This is obviously applicable only to geological objects much greater than a RVE. In most cases, crustal rocks heterogeneity is mainly the result of variable mineral composition and of the presence of pores and cracks. Effective Medium Theories (EMT) have been constructed that allow to successfully predict rock properties as long as the degree of heterogeneity is not large. There exists in general some critical threshold above which such an approach does not apply. The limits of application of EMT to rocks has been examined by Guéguen et al. (1997). We restrict ourselves in the following to the applicability field of EMT.

Use of EMT in order to predict elastic properties and hence elastic wave velocities is of direct interest. Elastic waves velocities are currently obtained from seismic and seismological data. The goal of Rock Physics is to extract from such data information on the physical state of the rock. In the oil industry, this has direct bearings on a quantification of the oil content and the identification of the fluid nature, *i.e.* oil or gas. In seismotectonics, an open question remains to know whether earthquakes can be predicted or not: elastic waves velocities variations have been considered as a possible precursory effect in that case.

In crustal conditions, all rocks contain cracks. Cracks represent an extremely small amount of porosity, typically less than 10^{-2}. Yet they have been identified for a long time as the major cause of elastic properties modifications (Simmons and Brace 1965; Walsh 1965). Their existence explains the differences observed between static and dynamic moduli, and also the elastic anisotropy of rocks which do not exhibit any mineral preferred orientation (Kern 1978; Sarout and Guéguen 2008a; Sarout and Guéguen 2008b). Because cracks are in general due to anisotropic stresses, crack orientation distribution is expected to be anisotropic. Reviews on cracked solids have been given by Kachanov (1992) or Kachanov (1993) who provide appropriate EMT methods to calculate anisotropic elastic properties of cracked rocks.

Yet elastic anisotropy of rocks is moderate in most cases, and the transversely isotropic (TI) symmetry is sufficient to describe it in general. This has led Thomsen (1986) to introduce three very convenient parameters to express the phase velocities of P, SV, SH waves in any plane containing the symmetry

axis. EMT calculations of anisotropic elastic properties provide a way to get Thomsen's parameters.

When fluids are present, frequency dependence is expected and the combined use of EMT methods and poroelasticity theory allow to account for it (Le Ravalec and Guéguen 1996). We focus in the following on elastic wave velocities in porous/cracked rocks and develop a method to derive theoretically Thomsen's parameters in the dry and saturated case. Frequency effects are calculated using both EMT and poroelasticity. We focus our attention to the case of a rock with isotropic matrix, *i.e.*, anisotropy is only due to the presence of cracks.

2 Effective Elastic Properties

We introduce in this section the basic results that are required to express elastic properties of cracked rocks. Following Kachanov (1993), we give the key relations that express effective elastic properties in terms of rock matrix elastic constants, fluid bulk modulus, and crack parameters. Because cracks are elastically compliant, we consider a single crack as a source of extra strain. This implies that EMT is used to calculate the extra compliance that is due to the presence of a crack. A stiffness approach would have to be considered if a stiff inclusion (source of extra stress) was present. Each of these two approaches - compliance and stiffness - is appropriate for either of the two cases: compliant or stiff inclusion.

2.1 A Single Crack

For a single pore, the extra strain per reference volume V due to its presence is an integral over the pore boundary

$$\Delta\boldsymbol{\epsilon} = \frac{1}{2V}\int(\mathbf{un} + \mathbf{nu})\mathrm{d}S, \tag{1}$$

where $\mathbf{u}$ is the displacement vector generated by applied stress $\boldsymbol{\sigma}$, and $\mathbf{n}$ the crack unit normal vector. For a crack, (1) reduces to

$$\Delta\boldsymbol{\epsilon} = \frac{1}{2V}\int([\mathbf{u}]\mathbf{n} + \mathbf{n}[\mathbf{u}])\mathrm{d}S, \tag{2}$$

where $[\mathbf{u}] = \mathbf{u}^+ - \mathbf{u}^-$ is the displacement discontinuity vector along the crack surface (the + side corresponds to the positive direction of $\mathbf{n}$).

For a *flat (planar)* crack, $\mathbf{n}$ is constant along S and

$$\Delta\boldsymbol{\epsilon} = \frac{S}{2V}(\mathbf{bn} + \mathbf{nb}), \tag{3}$$

where $\mathbf{b} =< \mathbf{u}^+ - \mathbf{u}^- >$ is the average, over S, displacement discontinuity vector.

Strains generated by a flat crack under remotely applied stress $\boldsymbol{\sigma}$ are given by (3); they are determined by $\mathbf{b}$, the average displacement discontinuity. A symmetric second rank crack compliance tensor $\mathbf{B}$ can be introduced that relates $\mathbf{b}$ to vector of uniform traction $\mathbf{n}\cdot\boldsymbol{\sigma}$ induced at the crack site (in a continuous material) by $\boldsymbol{\sigma}$

$$\mathbf{b} = \mathbf{n}\cdot\boldsymbol{\sigma}\cdot\mathbf{B}. \tag{4}$$

Relation (4), *i.e.*, introduction of tensor $\mathbf{B}$, is simply a statement of linearity of the system ($\mathbf{b}$ is a linear function of $\mathbf{n}\cdot\boldsymbol{\sigma}$). For the elastically axisymmetric crack shapes in an isotropic matrix

$$\mathbf{B} = B_N\ \mathbf{nn} + B_T\ \left(\mathbf{I} - \mathbf{nn}\right). \tag{5}$$

For a $3-D$ *circular crack* (dry case) of radius a (Kachanov 1993)

$$\begin{aligned} B_T^{dry} &= \frac{32\left(1-\nu_o^2\right)a}{3\pi E_o\left(2-\nu_o\right)}, \\ \frac{B_N^{dry}}{B_T^{dry}} &= 1 - \frac{\nu_o}{2}. \end{aligned} \tag{6}$$

where E_o and ν_o are the Young modulus and Poisson's ratio of the isotropic rock forming mineral, respectively.

The values of B_N^{dry} and B_T^{dry} are relatively close (the factor $\nu_o/2$ is of the order of 0.1 for $\nu_o = 0.25$, a typical value for rocks) and the deviation of the proportionality of $\mathbf{B}$ to $\mathbf{I}$ is relatively small.

We now focus on the saturated case of flat narrow cracks, and account for the fact that the normal compliances of a crack is changed due to fluid saturation. Specializing formulas of (Shafiro and Kachanov 1997) for the case of cracks, we obtain the fluid saturated values of B_N and B_T for a *circular crack* of radius a, that generalize formulas (6) for a dry crack

$$B_T^{sat} = \frac{32\left(1-\nu_o^2\right)\ a}{3\pi E_o\left(2-\nu_o\right)},$$
$$\frac{B_N^{sat}}{B_T^{sat}} = \left(1-\frac{\nu_o}{2}\right)\frac{\delta_f}{1+\delta_f}, \tag{7}$$

where the solid/fluid coupling parameter δ_f characterizes the coupling between the stress and the fluid pressure for a given spheroid of aspect ratio ζ. For a first-order spheroidal crack ($\zeta \ll 1$), δ_f is controlled by the crack aspect ratio

$$\delta_f^{crack} = \left[\frac{E_o}{K_f} - 3\left(1-2\nu_o\right)\right]\frac{\pi\zeta}{4\left(1-\nu_o^2\right)}, \tag{8}$$

where ζ is the crack aspect ratio ($\zeta = w/a$ where $2w$ is the crack average opening). In general, ζ is not the same for cracks of all sizes and orientations, therefore, δ_f^{crack} is generally different for different cracks. For instance, if a water-saturated crack ($K_f = 2.3$ GPa) of aspect ratio $\zeta = 10^{-3}$ is embedded in an isotropic matrix with $E_o = 70$ GPa and $\nu_o = 0.27$, then $\delta_f^{crack} \simeq 10^{-2}$. When $\delta_f^{crack} \to \infty$, we recover (6) from (7). This limit applies to a dry or gas-filled crack. Note that the other limit, *i.e.*, $\delta_f^{crack} \to 0$, is not physically possible. It would imply either a very stiff fluid ($K_f >> K_o = E_o/3\left(1-2\nu_o\right)$), or an infinitely thin crack ($\zeta \to 0$). The first case is out of the range of validity of the compliance approach (a stiff inclusion would require the use of the stiffness approach), while the second case implies a zero crack aperture, hence no fluid.

2.2 Multiple Cracks and Crack Induced Anisotropy

In this section, compliance contributions of cracks are evaluated in the non-interaction approximation, (NIA) without accounting for the interactions between cracks. Various approximate schemes, *e.g.*, self-consistent (Hill 1965; Budiansky and O'Connell 1976), differential (Vavakin and Salganik 1975; Bruner 1976; Hashin 1983; Le Ravalec and Guéguen 1996; Saenger 2007), and Mori-Tanaka's (Mori and Tanaka 1973; Benveniste 1987), account for interactions by making the effective constants as functions of the parameters defined in the NIA. As discussed by Kachanov (1993) and Grechka and Kachanov (2006), the NIA is valid over a broad range of crack densities. For multiple flat cracks in the NIA, the extra strain due to these cracks is simply the sum $\Delta\boldsymbol{\epsilon}=\frac{1}{2V}\sum\left[(\mathbf{bn}+\mathbf{nb})\,S\right]^{(m)}$, that may be replaced by integration over orientations if computationally convenient. The overall strain (per representative volume V containing cracks) can be represented as a sum

$$\begin{aligned}\boldsymbol{\epsilon} &= \boldsymbol{\epsilon}^o + \Delta\boldsymbol{\epsilon}, \\ &= \mathbf{S} : \boldsymbol{\sigma} = (\mathbf{S}^o + \Delta\mathbf{S}) : \boldsymbol{\sigma},\end{aligned} \tag{9}$$

where $\mathbf{S}$ are the effective compliances, $\mathbf{S}^o$ are the bulk material compliances (assumed to be isotropic here) and $\boldsymbol{\sigma}$ are the applied elastic stresses. Finding the effective compliances reduces to expressing extra strain $\Delta\boldsymbol{\epsilon}$ due to cracks in terms of applied stresses. For a single crack m, the fundamental quantity to be estimated is the *compliance contribution tensor*, a fourth-rank tensor such that the crack strain contribution $\Delta\boldsymbol{\epsilon}$ is

$$\begin{aligned}\Delta\boldsymbol{\epsilon}^{(m)} &= \Delta\mathbf{S}^{(m)} : \boldsymbol{\sigma}, \\ &= \mathbf{H}^{(m)} : \boldsymbol{\sigma}.\end{aligned} \tag{10}$$

The trace of this tensor $\mathrm{tr}\left(\mathbf{H}^{(m)} : \mathbf{I}\right) = H_{iijj}^{(m)}$ is the compressibility of the m^{th} pore: it was calculated by Zimmerman (1991) for a number of pore shapes of relevance to rocks. In the complete form, **H**-tensor was given, for a number of $2-D$ and $3-D$ pore shapes by Kachanov (1993). Then, for multiple cracks, in the NIA, we have

$$\Delta\boldsymbol{\epsilon} = \sum_m \mathbf{H}^{(m)} : \boldsymbol{\sigma}, \tag{11}$$

which identifies the fourth-rank tensor

$$\Delta\mathbf{S} = \mathbf{H} = \sum_m \mathbf{H}^{(m)}, \tag{12}$$

as the proper general damage parameter (tensorial crack density).

In the isotropic case, *i.e.*, isotropic background solid and randomly oriented circular cracks, the crack density parameter is the classical scalar

$$\rho = \frac{1}{V}\sum_m \left(a^3\right)^{(m)}, \tag{13}$$

where $a^{(m)}$ is the m^{th} crack radius. Note that the proportionality of the individual crack contributions to their sizes cubed corresponds to their actual contributions to the overall compliances. This parameter, introduced by Bristow (1960) in the context of materials science, and by Walsh (1965) in the geophysical context was extended to the elliptic planar cracks by Budiansky and O'Connell (1976). We examine in the following the general case of non-random crack orientations and crack-induced anisotropy. This requires generalization of the scalar crack density parameter, ρ, to a tensorial one. Indeed, for any flat crack, its contribution to the overall strain is given by **H**-tensor, that is expressed in terms of **B** using equations (3) and (4)

$$\Delta\mathbf{S} = \mathbf{H} = \frac{S}{V}\mathbf{nBn}, \tag{14}$$

or, in indicial notation

$$\Delta S_{ijkl} = \frac{S}{4V}\left[B_{ik}n_j n_l + B_{il}n_j n_k + B_{jk}n_i n_l + B_{jl}n_i n_k\right] \tag{15}$$

with symmetrization with respect to $ij \leftrightarrow kl, i \leftrightarrow j, k \leftrightarrow l$, imposed on $ijkl$ components. Therefore, for multiple flat cracks, the proper general crack density parameter is the fourth-rank tensor

$$\Delta\mathbf{S} = \mathbf{H} = \frac{1}{V}\sum_m (S\ \mathbf{nBn})^{(m)}. \tag{16}$$

Note that this last formula holds for flat cracks of arbitrary shapes, provided that $\mathbf{B}$ is known for the given shape.

2.3 Dry Cracks Compliances

We now consider dry circular cracks for which B_N and B_T are known to be different but relatively close from equation (6). From equations (6) and (16), the extra compliances are

$$\Delta S^{dry}_{ijkl} = \frac{32(1-\nu_o^2)}{3(2-\nu_o)E_o}\left[\frac{1}{4}(\delta_{ik}\alpha_{jl} + \delta_{il}\alpha_{jk} + \delta_{jk}\alpha_{il} + \delta_{jl}\alpha_{ik}) - \frac{\nu_o}{2}\beta_{ijkl}\right], \tag{17}$$

in terms of second- and fourth-rank damage tensors

$$\alpha_{ij} = \frac{1}{V}\sum_m \left(a^3\ n_i n_j\right)^{(m)}$$
$$\beta_{ijkl} = \frac{1}{V}\sum_m \left(a^3 n_i n_j n_k n_l\right)^{(m)} \tag{18}$$

where we note that in addition to second rank crack density tensor $\boldsymbol{\alpha}$, fourth rank tensor $\boldsymbol{\beta}$ emerges as a second crack density parameter. Note that

$$\beta_{ijqq} = \frac{1}{V}\sum_m \left(a^3 n_i n_j n_q n_q\right)^{(m)} = \frac{1}{V}\sum_m \left(a^3 n_i n_j\right)^{(m)} = \alpha_{ij},$$
$$\beta_{ppqq} = \frac{1}{V}\sum_m \left(a^3 n_p n_p n_q n_q\right)^{(m)} = \frac{1}{V}\sum_m \left(a^3\right)^{(m)} = \mathrm{tr}\left(\alpha_{ij}\right) = \rho. \tag{19}$$

Because of the small factor $\nu_o/2$, one may note that the $\boldsymbol{\beta}$-term contribution is small in the dry case. However, retaining $\boldsymbol{\alpha}$ as the sole crack density parameter is not a very good approximation and may be misleading.

Of particular interest for geophysical applications is the case of transverse isotropy (TI), or hexagonal, symmetry; in the text to follow, we choose x_3 as the axis of symmetry. This covers two main orientation distributions of cracks (or any combination of both):

(i) Approximately parallel cracks, all perpendicular to x_3. This case is relevant, for example, for foliated rocks where cracks are almost exactly parallel. Then $\alpha_{11} = \alpha_{22} = 0$ and $\alpha_{33} \neq 0$;

(ii) Cracks with normals randomly oriented in plane x_1x_2. Then $\alpha_{11} = \alpha_{22} \neq 0$ and $\alpha_{33} = 0$. This case is relevant to rocks undergoing deviatoric tectonic stresses.

In both cases, $\alpha_{11} = \alpha_{22}$, in agreement with the condition $2\Delta S^{dry}_{1212} = (\Delta S^{dry}_{1111} - \Delta S^{dry}_{1122})$ imposed by transversely isotropic symmetry (Nye 1979). Note that $\boldsymbol{\beta}$ is symmetric with respect to all rearrangements of indices, *e.g.*, $\beta_{1133} = \beta_{1313} = \beta_{2233} = \beta_{2323}$, $\beta_{1122} = \beta_{1212}$. Therefore we have

$$
\begin{aligned}
S^{dry}_{1111} &= S^{dry}_{2222} = \frac{1}{E_o} + h\left(\alpha_{11} - \frac{\nu_o}{2}\beta_{1111}\right),\\
S^{dry}_{3333} &= \frac{1}{E_o} + h\left(\alpha_{33} - \frac{\nu_o}{2}\beta_{3333}\right),\\
S^{dry}_{1133} &= S^{dry}_{2233} = S^{dry}_{3311} = -\frac{\nu_o}{E_o} - \frac{\nu_o}{2}\beta_{1133},\\
S^{dry}_{1212} &= \frac{S^{dry}_{1111} - S^{dry}_{1122}}{2} = \frac{1+\nu_o}{2E_o} + \frac{h}{2}\left(\alpha_{11} - \frac{\nu_o}{3}\beta_{1111}\right),\\
S^{dry}_{1313} &= S^{dry}_{3232} = \frac{1+\nu_o}{2E_o} + \frac{h}{4}(\alpha_{11} + \alpha_{33} - 2\nu_o\beta_{1133}),
\end{aligned}
\tag{20}
$$

where

$$
h = \frac{32(1-\nu_o^2)}{3(2-\nu_o)E_o}. \tag{21}
$$

2.4 High Frequency Compliances of Fluid-Saturated Cracks

This section focuses on fluid-saturated rocks. The presence of a liquid instead of air "stiffens" cracks and thus may strongly affect their compliance contributions. Crack density parameters need to be modified; in particular, crack aspect ratios, albeit small, become important factors, since they control the

stiffening effect of the fluid. One of the consequences is that the fourth-rank tensor $\boldsymbol{\beta}$ starts to play an important role.

In the following, the fluid is assumed to be linearly compressible, with bulk modulus K_f. We also assume that δ_f and ζ can be approximately considered as identical for all cracks. It would be, of course, more satisfactory to introduce a distribution of ζ values. However, the lack of appropriate, reliable data, on such distributions on actual rocks prevents, in general, from using a more complete theory. Then equation (17) is modified into

$$\begin{aligned}\Delta S^{sat}_{ijkl} = h \Big[& \frac{1}{4} \left(\delta_{ik}\alpha_{jl} + \delta_{il}\alpha_{jk} \right. \\ & \left. + \delta_{jk}\alpha_{il} + \delta_{jl}\alpha_{ik} \right) \\ & + \psi \beta_{ijkl} \Big] ,\end{aligned} \tag{22}$$

where α_{ij} and β_{ijkl} in the fluid-saturated case are still given by (18). Tensor $\boldsymbol{\beta}$ in the saturated case enters now with multiplier

$$\psi = (1 - \frac{\nu_o}{2}) \frac{\delta_f}{1 + \delta_f} - 1, \tag{23}$$

instead of $-\nu_o/2$ in the dry case. In the isotropic case (random crack orientations, $\alpha_{ij} = (\rho/3)\delta_{ij}$) this formula recovers results of Budiansky and O'Connell (1976). We emphasize that the compliances given by (22) are unrelaxed compliances, *i.e.*, no fluid flow occurs at a local scale between neighbor pores (see section 2.5). These unrelaxed compliances are relevant at high frequencies. It makes the difference with the dry case, *i.e.*, B^{sat}_N and B^{sat}_T are substantially different, making the $\boldsymbol{\beta}$-tensor terms non-negligible. In the TI case (the most frequent anisotropic case in geophysics), the number of independent elastic constants is five (full, non-elliptic TI symmetry), each of them depends on seven parameters (E_o, ν_o, two $\boldsymbol{\alpha}$ components, and three $\boldsymbol{\beta}$ components). Indeed, for a general TI orientation distribution of cracks, $\alpha_{11} = \alpha_{22}$, $\beta_{1111} = \beta_{2222}$, $\beta_{1212} = \beta_{1122} = \beta_{1111}/3$. Recall that $\boldsymbol{\beta}$ may further be simplified since it is symmetric with respect to all rearrangement of indices, implying that $\beta_{1313} = \beta_{1133} = \beta_{2323} = \beta_{2233}$, and leaving only three non-zero β_{ijkl} components. For this fluid-saturated case, equations (20) become

$$
\begin{aligned}
S^{sat}_{1111} &= S^{sat}_{2222} = \frac{1}{E_o} + h\left(\alpha_{11} + \psi\beta_{1111}\right), \\
S^{sat}_{3333} &= \frac{1}{E_o} + h\left(\alpha_{33} + \psi\beta_{3333}\right), \\
S^{sat}_{1133} &= S^{sat}_{2233} = S^{sat}_{3311} = -\frac{\nu_o}{E_o} + h\psi\beta_{1133}, \\
S^{sat}_{1212} &= \frac{S^{sat}_{1111} - S^{sat}_{1122}}{2} = \frac{1+\nu_o}{2E_o} + \frac{h}{2}\left(\alpha_{11} + \frac{\psi}{3}\beta_{1111}\right), \\
S^{sat}_{1313} &= S^{sat}_{3232} = \frac{1+\nu_o}{2E_o} + \frac{h}{4}\left(\alpha_{11} + \alpha_{33} + 4\psi\beta_{1133}\right),
\end{aligned}
\tag{24}
$$

where we note that these high frequency compliances S_{ijkl} depend on α_{ij} and β_{ijkl} components in a linear fashion. Note that for identical spheroidal cracks, the crack porosity ϕ is related to the crack density ρ and average aspect ratio ζ by

$$\phi = \frac{4}{3}\pi\rho\zeta. \tag{25}$$

Crack porosity is useful only in the water-saturated case, for spheroidal cracks. Although such a case of identical spheroids can only be an approximation for real rocks, it allows to point out the fact that, for a given porosity, crack density ρ and aspect ratio ζ cannot be described independently since $\zeta = 3\phi/4\pi\rho$ Sarout and Guéguen (2008b).

2.5 Effective Elasticity and Poroelasticity

The effective elasticity of fluid-saturated rocks with cracks and pores depends on the ratio between the rate of loading and the rate of fluid diffusion in the rock. In the context of wave propagation, this means dependence on the frequency. In order to illustrate this effect, we consider two limiting cases. The first one is such that within any Representative Volume Element (RVE), an equilibrium isobaric situation exists (identical fluid pressure in all pores and cracks as resulting from local flow). The second one corresponds to a state where no local flow at all takes place, so that pores and cracks, in a given RVE, have different fluid pressures.

At this point, it is important to discuss some basic results of Biot's theory of poroelasticity (Biot 1941; Biot 1956a; Biot 1956b; Guéguen et al. 2004). The key point is that only the first of the above mentioned situations (isobaric RVE) is within the scope of this theory. Indeed, poroelastic theory considers the porous/cracked rock as a continuous medium where, locally, all quantities are defined by averaging over the RVE. Pores and cracks are assumed to be interconnected and fluid pressure is defined over a RVE. Each mathematical point of the equivalent continuous medium represents a RVE.

2.5.1 Relaxed (isobaric) Compliances, Drained and Undrained

Let us first assume the isobaric condition for the fluid within any RVE so that Biot's theory of poroelasticity applies (*isobaric RVE, relaxed compliances*). Poroelasticity defines in that case two types of compliances, the drained and undrained ones.

The *drained* compliances, $\mathbf{S}^d$, correspond to a deformation where each point of the equivalent continuous medium is subject to a constant fluid pressure (through connection to some reservoir). However, its fluid mass varies (through exchange with the reservoir). As a consequence, flow takes place over a macroscopic scale such as the wavelength scale. This assumes a quasi-static deformation because fluid diffusivity d in most rocks is typically small (fluid diffuses over the scale l in a time $\tau \sim l^2/d$). For example, for a wavelength $l \approx 5$ m (frequency in the seismic kHz range), and a diffusivity $d \approx 10^{-2}$ m^2.s^{-1} (typical for water in a sandstone of permeability 0.01 Darcy and shear modulus 10^{10} Pa, see Guéguen and Palciauskas (1994)), this implies that $\tau \approx 10^3$ s, a very large time period compared to the wave period. Thus, no macroscopic flow takes place during a wave period, and, as a consequence, the drained compliances are not those that are reflected in wavespeeds. The conclusion seems to be that drained compliances can be measured in quasi-static fluid-saturated deformation conditions only. However, since linear poroelasticity ignores any pressure dependence of compliances (it is a linear theory, compliances are constant quantities), a simple way to measure the drained compliances is to use *dry* rock samples, in which case fluid pressure is $p_f = 0$. The "drained" compliances of poroelasticity $\mathbf{S}^d$ are thus identical to the "dry" compliances of effective elasticity $\mathbf{S}^{dry}$, *i.e.*, $\mathbf{S}^d = \mathbf{S}^{dry}$.

The *undrained* compliances, $\mathbf{S}^u$, of poroelasticity correspond to the opposite situation, a deformation where each point of the equivalent continuous medium has a constant fluid mass and its fluid pressure varies as a consequence of stress variations. There is no macroscopic fluid flow between RVE's but the pressure varies from one point of the equivalent continuous medium to another. This means that any RVE is in the isobaric state, but the fluid pressure varies from one RVE to another. Such a situation corresponds well to the example considered above, where a 5 m wavelength perturbation propagates through the medium. The wavespeeds "see" the undrained compliances because no macroscopic fluid flow can possibly take place. Undrained compliances are measured under any conditions where there is not enough time for the macroscopic flow to occur, and yet enough time for local flow to occur (at the RVE scale). But, if wavespeed measurements are performed at ultrasonic frequencies, typical of laboratory experiments, the RVE is not isobaric. In such a situation, high frequency unrelaxed compliances $\mathbf{S}^{sat}_{high}$ are extracted, which are different from the undrained compliances $\mathbf{S}^u = \mathbf{S}^{sat}_{low}$.

Note also that Biot-Gassmann (isotropic porous medium) and Brown-Korringa (anisotropic porous medium) relations are useful for prediction of undrained compliances $\mathbf{S}^u$ from drained $\mathbf{S}^d$ ones (Biot 1941; Gassman 1951; Brown and Korringa 1975; Schubnel and Guéguen 2003).

2.5.2 Unrelaxed Compliances

The case "*non-isobaric RVE, unrelaxed compliances*" is out of the validity range of Biot's theory of poroelasticity since fluid pressure is variable within a RVE. Of course, it is well within the validity range of the concept of effective elasticity since stresses and strains can be averaged in spite of non-uniformity of fluid pressure in RVE. Fluid pressures in pores or cracks of different shapes and orientations are different (pressure polarization), since there is not enough time for local fluid flow. Above a certain critical frequency, any experimental measurement of wavespeeds corresponds to this non-isobaric situation. There exists a transition domain between "low" and "high" frequency regimes.

The pressure polarization is coupled with the effective elastic properties of the RVE. An important observation is that, in the limit of narrow, crack-like pores, their (small) aspect ratios start to play an important role (in contrast with the dry rock, where they do not matter): they determine the stiffening effect of fluid.

The question is now: at what frequency f_c does the "pressure polarization" start to become noticeable enough? In fluid saturated cracked rocks, squirt flow at a microscopic scale is responsible for the frequency dependence of the elastic wave velocities. Ultrasonic measurements in the laboratory provide *high frequency* (MHz) values of the velocities (*unrelaxed compliances* $\mathbf{S}^{sat}_{high}$), whereas field data (seismology and seismics) correspond in general to *low frequency* (kHz - Hz) values (*relaxed compliances* $\mathbf{S}^{sat}_{low}$). The low frequency values are, as discussed above, the relaxed *undrained* quantities of poroelastic theory, *i.e.*, $\mathbf{S}^u = \mathbf{S}^{sat}_{low}$ (but, of course, the high frequency values are not the relaxed *drained* ones $\mathbf{S}^{sat}_{high} \neq \mathbf{S}^d$). The high frequency unrelaxed compliances $\mathbf{S}^{sat}_{high}$ obtained in the laboratory are not the relaxed compliances measured at the field scale $\mathbf{S}^u = \mathbf{S}^{sat}_{low}$, because of local flow at a microscopic scale (within a RVE). The critical frequency of maximum dissipation due to this local fluid flow f_c is obtained by calculating the time needed for local fluid motion between two neighbor cracks, as due to local pressure gradients (Le Ravalec and Guéguen 1996)

$$f_c \approx \zeta^3 E_o / 20\eta \tag{26}$$

where typically crack aspect ratio $\zeta \approx 10^{-3}$, sandstone Young's modulus $E_o \approx$ 70 GPa, fluid viscosity $\eta \approx 10^{-3}$ Pa.s, so that $f_c \approx 3.5$ kHz.

2.6 Low Frequency Compliances of Fluid-Saturated Cracks

Using equations (17), (22) and Brown-Korringa relations for the saturated transversely isotropic cracked rock yields

$$S_{ijkl}^{high} - S_{ijkl}^{low} = h\left[\left(\psi + \frac{\nu_o}{2}\right)\beta_{ijkl} + h\frac{\left(\alpha_{ij} - \frac{\nu_o}{2}\beta_{ijqq}\right)\left(\alpha_{kl} - \frac{\nu_o}{2}\beta_{ppkl}\right)}{\left(\frac{1}{K_{dry}} - \frac{1}{K_o}\right) + \phi\left(\frac{1}{K_f} - \frac{1}{K_o}\right)}\right],$$
$$S_{ijkl}^{high} - S_{ijkl}^{low} = h\left[\left(\psi + \frac{\nu_o}{2}\right)\beta_{ijkl} + \left(1 - \frac{\nu_o}{2}\right)\frac{\alpha_{ij}\alpha_{kl}}{(1+\delta_f)\,\mathrm{tr}\,(\alpha_{ij})}\right], \quad (27)$$

where ϕ is the crack porosity defined in (25). Note that this relation is different from that given in (Schubnel and Guéguen 2003). This latter was calculated by neglecting the $\boldsymbol{\beta}$-terms in the dry case. Such an approximation introduces errors that are significant when dispersion effects are investigated.

Therefore, low frequency elastic compliances are directly extracted from high frequency compliances measured in the laboratory at ultrasonic frequencies in both dry and fluid-saturated conditions. In the transversely isotropic cracked rock configuration, (27) translates to

$$S_{1111}^{low} = S_{1111}^{high} - h\left[\left(\psi + \frac{\nu_o}{2}\right)\beta_{1111} + \left(1 - \frac{\nu_o}{2}\right)\frac{\alpha_{11}^2}{(1+\delta_f)\,(2\alpha_{11} + \alpha_{33})}\right],$$
$$S_{3333}^{low} = S_{3333}^{high} - h\left[\left(\psi + \frac{\nu_o}{2}\right)\beta_{3333} + \left(1 - \frac{\nu_o}{2}\right)\frac{\alpha_{33}^2}{(1+\delta_f)\,(2\alpha_{11} + \alpha_{33})}\right],$$
$$S_{1133}^{low} = S_{1133}^{high} - h\left[\left(\psi + \frac{\nu_o}{2}\right)\beta_{1133} + \left(1 - \frac{\nu_o}{2}\right)\frac{\alpha_{11}\alpha_{33}}{(1+\delta_f)\,(2\alpha_{11} + \alpha_{33})}\right], \quad (28)$$
$$S_{1212}^{low} = S_{1212}^{high} - h\left[\left(\psi + \frac{\nu_o}{2}\right)\frac{\beta_{1111}}{3}\right],$$
$$S_{1313}^{low} = S_{1313}^{high} - h\left[\left(\psi + \frac{\nu_o}{2}\right)\beta_{1133}\right],$$

where the reference frame (x_1, x_2, x_3) coincides with the principal axes of the crack density tensor $\boldsymbol{\alpha}$ such that $\alpha_{12} = \alpha_{13} = 0$.

Further, in the fluid-saturated case for which a difference between high and low frequency compliances exists, and using relations (24) for estimating S_{ijkl}^{high} components, we get

$$
\begin{aligned}
S^{low}_{1111} &= \frac{1}{E_o} + h\left[\alpha_{11} - \frac{\nu_o}{2}\beta_{1111} - \left(1-\frac{\nu_o}{2}\right)\frac{\alpha_{11}^2}{(1+\delta_f)(2\alpha_{11}+\alpha_{33})}\right],\\
S^{low}_{3333} &= \frac{1}{E_o} + h\left[\alpha_{33} - \frac{\nu_o}{2}\beta_{3333} - \left(1-\frac{\nu_o}{2}\right)\frac{\alpha_{33}^2}{(1+\delta_f)(2\alpha_{11}+\alpha_{33})}\right],\\
S^{low}_{1133} &= -\frac{\nu_o}{E_o} - h\left[\frac{\nu_o}{2}\beta_{1133} + \left(1-\frac{\nu_o}{2}\right)\frac{\alpha_{11}\alpha_{33}}{(1+\delta_f)(2\alpha_{11}+\alpha_{33})}\right],\\
S^{low}_{1212} &= \frac{1+\nu_o}{2E_o} + \frac{h}{2}\left[\alpha_{11} - \frac{\nu_o}{3}\beta_{1111}\right],\\
S^{low}_{1313} &= \frac{1+\nu_o}{2E_o} + \frac{h}{2}\left[\frac{\alpha_{11}+\alpha_{33}}{2} - \nu_o\beta_{1133}\right],
\end{aligned}
\tag{29}
$$

where we note that unlike high frequency compliances S^{high}_{ijkl}, low frequency compliances S^{low}_{ijkl} depend on α_{ij} and β_{ijkl} components in a non-linear fashion.

3 Elastic Wave Velocities and their Anisotropy

In the *dry case*, wavespeeds are controlled by quasi-static effective elastic properties. Both field and laboratory data are in the validity domain of linear elasticity, *i.e.*, they are both low strain amplitudes measurements. Both provide quasi-static effective properties that can be directly compared.

However, measurements in the *saturated case* exhibit frequency dependence (dispersion). The low frequency (quasi-static) regime extends up to a critical frequency f_c in this case. Only above f_c are measured high frequency effective elastic properties. This implies that laboratory (high frequency) data cannot be directly compared to field (low frequency) data. However, using poroelastic theory makes it possible to compare them, as discussed in sections 2.5 and 2.6.

3.1 Anisotropy and Thomsen's Parameters

Thomsen introduced three dimensionless parameters, ε, γ and δ, that characterize the extent of anisotropy in a way suitable for geophysical applications of elastic theory. He concentrated on TI media, the most frequent case in geophysics, for which five independent elastic constants are needed. The three parameters ε, γ and δ, together with the velocities $V_P^o = \sqrt{C_{33}/\rho}$ and $V_S^o = \sqrt{C_{44}/\rho}$, where ρ is the rock density, characterize TI elastic properties in a way equivalent to the five independent elastic constants C_{11}, C_{33}, C_{13}, C_{44} and C_{66} in Voigt's two-index notation for instance. Thomsen's parameters allow us to discriminate the isotropic contribution V_P^o and V_S^o to the over

all elastic properties from the deviation of these properties, ε, γ and δ, from isotropy. Thomsen's anisotropy parameters are defined as

$$\begin{aligned}\varepsilon &= \frac{C_{11}-C_{33}}{2C_{33}}, \quad \gamma = \frac{C_{66}-C_{44}}{2C_{44}},\\ \delta &= \frac{(C_{13}+C_{44})^2-(C_{33}-C_{44})^2}{2C_{33}(C_{33}-C_{44})}.\end{aligned} \tag{30}$$

where stiffnesses C_{ij} in Voigt's two-index notation are obtained from the tensorial inversion of the elastic compliances S_{ijkl} given by (20), (24) or (29)

The so-called anellipticity parameter $\eta = (\varepsilon-\delta)/(1+2\delta)$ quantifies the departure of the wave front from an ellipsoidal shape. Thomsen's parameters cancel in the case of isotropy; if all of them are much smaller than 1, the anisotropy is considered to be weak, in the sense of low amplitude of anisotropy within a given symmetry group such as transverse isotropy (hexagonal symmetry). Within this approximation, the angular variations of the phase velocities, in any plane containing the symmetry axis x_3, are given by approximate relations obtained from Taylor's expansion to the first order in terms of the small quantities ε, γ and δ, *i.e.*,

$$\begin{aligned}V_P(\theta) &\approx V_P^o(1+\delta\sin^2\theta\cos^2\theta+\varepsilon\sin^4\theta),\\ V_{SV}(\theta) &\approx V_S^o\left(1+\left(\frac{V_P^o}{V_S^o}\right)^2(\varepsilon-\delta)\sin^2\theta\cos^2\theta\right),\\ V_{SH}(\theta) &\approx V_S^o(1+\gamma\sin^2\theta),\end{aligned} \tag{31}$$

where θ is the phase angle between the wave-front normal and the TI axis x_3. There are two shear waves, denoted by SH for the pure shear wave polarized perpendicularly to x_3 and SV for the pseudo-shear wave polarized normal to the SH polarization. Note that the case $\eta = 0$, *i.e.*, $\varepsilon = \delta$ corresponds to $V_{SV}(\theta) \approx V_S^o$ and $V_P(\theta) \approx V_P^o(1+\delta\sin^2\theta)$. For the case $\eta = 0$, any wave front propagating in a plane containing x_3 is elliptic, *i.e.*, both $V_P(\theta)$ and $V_{SH}(\theta)$ have a $\sin^2(\theta)$ dependence.

3.2 Elastic Anisotropy of a Dry Cracked Medium

In that case, no frequency dependence of elastic wave velocities is expected. We consider now the crack-induced anisotropy of a dry rock given by equations (17) or (20). Two cases are detailed in this section, the approximate (β_{ijkl} terms neglected) and the complete dry solutions.

In the approximate dry solution, the overall anisotropy is transverse isotropy

of the simplified type, where five constants (V_P^o, V_S^o, ε, γ and δ) reduce to four independent ones (V_P^o, V_S^o, γ and $\varepsilon = \delta$), that depend on four microstructural parameters, *i.e.*, α_{11}, $\alpha_{22} = \alpha_{33}$, E_o and ν_o. The obvious question is then: what are the relations between the three Thomsen's parameters ε, γ and δ on one hand, and the four parameters (E_o, ν_o, α_{11}, α_{33}) on the other hand ? Using either E_o, ν_o or $S_{11}^o = 1/E_o, S_{12}^o = -\nu_o/E_o$, (Voigt's notation), one obtains

$$\varepsilon_{dry} = \delta_{dry} = \frac{h(\alpha_{33} - \alpha_{11})(1/E_o + h\alpha_{11})}{2\left[(1+\nu_o)/E_o + h\alpha_{11}\right]\left[(1-\nu_o)/E_o + h\alpha_{11}\right]}, \tag{32}$$

and

$$\gamma_{dry} = \frac{h\left(\alpha_{33} - \alpha_{11}\right)}{4\left[(1+\nu_o)/E_o + h\alpha_{11}\right]}. \tag{33}$$

In this case, anellipticity $\eta = 0$ and any wave front propagating in a vertical plane containing x_3 is elliptic (Thomsen 1986). Such a simplification is of interest in seismics. One sees from (32) and (33) that Thomsen's parameters are in that case a direct measure of α_{11} and α_{33} if the matrix elastic constants E_o and ν_o are known. A further simplification occurs in the case where either α_{11} or α_{33} vanishes (for example one set of parallel cracks).

In the complete dry solution, the overall anisotropy is general transverse isotropy, characterized by five independent elastic constants, that depend on seven microstructural parameters, i.e., α_{11}, $\alpha_{22} = \alpha_{33}$, β_{1111}, β_{3333}, β_{1133}, E_o and ν_o. Equations (17) or (20) allows us to explicit the relationship between ε, γ and δ and those microstructural parameters, i.e.,

$$\begin{aligned}
\varepsilon_{dry} &= \frac{a_o + a_1\psi_d + a_2\psi_d^2}{b_o + b_1\psi_d + b_2\psi_d^2}, \\
\delta_{dry} &= \frac{c_o + c_1\psi_d + c_2\psi_d^2 + c_3\psi_d^3}{d_o + d_1\psi_d + d_2\psi_d^2 + d_3\psi_d^3},
\end{aligned} \tag{34}$$

and

$$\gamma_{dry} = \frac{h\left[3\left(\alpha_{33} - \alpha_{11}\right) - 4\psi_d\left(\beta_{1111} - 3\beta_{1133}\right)\right]}{12\left[(1+\nu_o)/E_o + h\alpha_{11}\right] + 8h\psi_d\beta_{1111}}, \tag{35}$$

where

$$\psi_d = -\frac{\nu_o}{2}, \tag{36}$$

and

$$
\begin{aligned}
a_o &= 9E_o h(1+E_o h\alpha_{11})(\alpha_{11}-\alpha_{33}),\\
a_1 &= 3E_o h[(3+2\nu_o+6E_o h\alpha_{11}-3E_o h\alpha_{33})\beta_{1111}\\
&\quad -3(2\nu_o\beta_{1133}+(1+E_o h\alpha_{11})\beta_{3333})],\\
a_2 &= E_o^2h^2\left[8\beta_{1111}^2+9\left(\beta_{1133}^2-\beta_{1111}\beta_{3333}\right)\right],\\
b_o &= 18\left[\nu_o^2-(1+E_o h\alpha_{11})^2\right],\\
b_1 &= -12E_o h(3+\nu_o+3E_o h\alpha_{11})\beta_{1111},\\
b_2 &= -16E_o^2h^2\beta_{1111}^2,\\
c_o &= -9E_o h(1+E_o h\alpha_{11})^2(\alpha_{33}-\alpha_{11}),\\
c_1 &= 6E_o h(1+E_o h\alpha_{11})[9\beta_{1133}-3\beta_{3333}+E_o h[4\left(\alpha_{11}-\alpha_{33}\right)\beta_{1111},\\
&\quad +3\left(2\alpha_{11}+\alpha_{33}\right)\beta_{1133}-3\alpha_{11}\beta_{3333}]+\nu_o\left[4\beta_{1111}+3(\beta_{3333}-7\beta_{1133})\right]]\\
c_2 &= E_o^2h^2[[2\nu_o(4\beta_{1111}-3\beta_{1133})(4\beta_{1111}+3(\beta_{3333}-7\beta_{1133}))\\
&\quad +6(4\beta_{1111}(5\beta_{1133}-2\beta_{3333})+3\beta_{1133}(\beta_{1133}+\beta_{3333})]\\
&\quad +E_o h[-\alpha_{33}(4\beta_{1111}-3\beta_{1133})^2\\
&\quad +\alpha_{11}(16\beta_{1111}^2+96\beta_{1111}\beta_{1133}+27\beta_{1133}^2-48\beta_{1111}\beta_{3333}+18\beta_{1133}\beta_{3333})]],\\
c_3 &= 8E_o^3h^3(4\beta_{1111}-3\beta_{1133})\left[2\beta_{1111}\beta_{1133}+3\beta_{1133}^2-\beta_{1111}\beta_{3333}\right],\\
d_o &= 18\left(1+E_o h\alpha_{11}\right)\left[\nu_o^2-(1+E_o h\alpha_{11})^2\right],\\
d_1 &= -6E_o h[8\left[\nu_o\left(1-\nu_o+E_o h\alpha_{11}\right)+(1+E_o h\alpha_{11})^2\right]\beta_{1111}\\
&\quad -3(1-\nu_o+E_o h\alpha_{11})[(1-\nu_o+E_o h\alpha_{11})\beta_{3333}\\
&\quad -4((1-2\nu_o)+E_o h\alpha_{11})\beta_{1133}]],\\
d_2 &= -4E_o^2h^2[8(1+2\nu_o+E_o h\alpha_{11})\beta_{1111}^2+9(1-\nu_o+E_o h\alpha_{11})\beta_{1133}^2\\
&\quad -12\beta_{1111}\left[(1-\nu_o+E_o h\alpha_{11})\beta_{3333}-4((1-2\nu_o)+E_o h\alpha_{11})\beta_{1133}\right]],\\
d_3 &= -16E_o^3h^3\beta_{1111}\left(8\beta_{1111}\beta_{1133}+3\beta_{1133}^2-2\beta_{1111}\beta_{3333}\right),
\end{aligned}
\tag{37}
$$

Figure 1 illustrates the predicted evolutions of anisotropy parameters ε_{dry}, γ_{dry} and δ_{dry} as a function of damage parameters $\mathrm{tr}(\boldsymbol{\alpha})/\Delta\alpha_o = (2\ \alpha_{11}+\alpha_{33})/\Delta\alpha_o$ and $\Delta\alpha/\mathrm{tr}(\alpha_o) = (\alpha_{33}-\alpha_{11})/\mathrm{tr}(\alpha_o)$ in a dry cracked rock of general TI symmetry. Calculations using the full equation (17) or (20) (without neglecting β_{ijkl} terms) are given in plain lines, while dashed lines show the results of the approximated solution (β_{ijkl} terms neglected) given explicitly in (32) and (33). Note that for a given matrix E_o and ν_o, Thomsen's parameters depend only on $\mathrm{tr}(\boldsymbol{\alpha})$ and $\Delta\alpha$ in the approximate dry solution (β_{ijkl} terms neglected $\equiv$ elliptic transverse isotropy), while it also depends on β_{1111}, β_{3333} and β_{1133} in the complete dry solution.

The values of damage parameters β_{1111}, β_{3333} and β_{1133} used in the theoretical predictions of anisotropy for a dry cracked rock have been obtained from Schubnel et al. (2003), a data set obtained from a granite sample submitted to deviatoric stresses. The corresponding values of $\mathrm{tr}(\alpha)$ and $\Delta\alpha$ are reported in Table 1, and solid elastic parameters are $E_o = 70$ GPa and $\nu_o = 0.27$.

Direct quantitative observations on predicted anisotropy evolutions in a dry cracked rock for the general TI symmetry can be made: (i) $\varepsilon_{dry} = \delta_{dry}$ and γ_{dry} increase with increasing $\Delta\alpha = \alpha_{33} - \alpha_{11}$ at fixed $\mathrm{tr}(\alpha) = 2\ \alpha_{11} + \alpha_{33}$; (ii) $\varepsilon_{dry} = \delta_{dry}$ and γ_{dry} decrease with increasing $\mathrm{tr}(\alpha) = 2\ \alpha_{11} + \alpha_{33}$ at fixed $\Delta\alpha = \alpha_{33} - \alpha_{11}$; (iii) γ_{dry} is always smaller than ε_{dry} for horizontal cracks; and (iv) negative values for ε, γ and δ are obtained for vertical cracks.

3.3 Validity of the Approximation Neglecting β_{ijkl} Terms

It is possible to discuss further the validity of the approximation made when neglecting β_{ijkl} terms. In the approximation, transverse isotropy is elliptic ($\varepsilon_{dry}^{approx} = \delta_{dry}^{approx}$). A complete calculation (with β_{ijkl} terms in the saturated case as shown in equation (24) and section 3.4) shows that in dry conditions ($K_f \to 0$ or $\delta_f^{crack} \gg 1$), ε_{dry} and δ_{dry} remain distinct although the difference is small (Figure 2). Depending on the resolution of the data, such a difference may or may not be visible.

Moreover, if dry data are used for direct microstructural interpretation (crack density in dry case), this approximation has been shown to be satisfactory. However, when dispersion effects are to be estimated through Biot-Gassman or Brown-Korringa relations, this approximation turns out to be too rough, and the $\boldsymbol{\beta}$-terms are required.

3.4 Elastic Anisotropy of a Fluid-Saturated Cracked Medium

Although we consider, as in the previous section, a TI medium with an isotropic matrix, the saturated situation is more complex for two reasons. First we have five independent elastic constants, each depending on seven parameters (two elastic constants of the matrix, two α_{ij} components, and three β_{ijkl} components). Then, low frequency compliances are given by $S^u_{ijkl} = S^{low}_{ijkl}$, that are different from the high frequency effective compliances S^{high}_{ijkl} and need to be calculated from them as shown in section 2.6.

The values of damage parameters α_{11}, α_{33}, β_{1111}, β_{1133}, β_{3333} used in the theoretical predictions of anisotropy for a fluid-saturated cracked rock have been taken from Schubnel et al. (2003) on a water-saturated Oshima granite. Those values are reported in Table 1, and for Oshima granite, solid elastic parameters are $E_o = 70$ GPa and $\nu_o = 0.27$. Water bulk modulus is $K_f = 2.3$ GPa and cracks porosity $\phi_o \simeq 0.2\%$.

3.4.1 Unrelaxed Elastic Properties and Anisotropy: Laboratory Investigations

Figure 3 (plain curves) illustrates the predicted evolution of anisotropy parameters ε_{sat}^{high}, γ_{sat}^{high} and δ_{sat}^{high} as a function of damage parameters $\mathrm{tr}(\alpha)/\Delta\alpha_o$, $\Delta\alpha/tr\,(\alpha_o)$, fluid bulk modulus K_f and cracks porosity ϕ, in a fluid-saturated cracked rock of general TI symmetry. Those anisotropies are calculated from the combined use of the inverted high frequency compliances S_{ijkl}^{high} as given by (24) and relations (30), *i.e.*,

$$\begin{aligned}\varepsilon_{sat}^{high} &= \frac{a_o + a_1\psi + a_2\psi^2}{b_o + b_1\psi + b_2\psi^2},\\ \delta_{sat}^{high} &= \frac{c_o + c_1\psi + c_2\psi^2 + c_3\psi^3}{d_o + d_1\psi + d_2\psi^2 + d_3\psi^3},\end{aligned} \tag{38}$$

with

$$\gamma_{sat}^{high} = \frac{h\left[3\left(\alpha_{33} - \alpha_{11}\right) - 4\psi\left(\beta_{1111} - 3\beta_{1133}\right)\right]}{12\left(\left(1+\nu_o\right)/E_o + h\alpha_{11}\right) + 8h\psi\beta_{1111}}, \tag{39}$$

where ψ is given by (23), and the a_i, b_i, c_i and d_i by (37). The high frequency predictions show that: (i) $\varepsilon_{sat}^{high} \neq \delta_{sat}^{high}$, which means that there is no ellipticity of the wave front; (ii) $\delta_{sat}^{high} > \varepsilon_{sat}^{high} > \gamma_{sat}^{high}$, with negative values possible for ε_{sat}^{high} and γ_{sat}^{high}; and (iii) the variation of ε_{sat}^{high} and γ_{sat}^{high} with K_f (and consequently saturation) is small, but there is a possible strong variation of δ_{sat}^{high} with K_f (depending on $\Delta\alpha$).

3.4.2 Relaxed Elastic Properties and Anisotropy: Field Applications (Seismics, Seismology)

Figure 3 (dashed curves) illustrates the predicted evolution of Thomsen's anisotropy parameters ε_{sat}^{low}, γ_{sat}^{low} and δ_{sat}^{low} as a function of damage parameters $\mathrm{tr}(\alpha) = 2\ \alpha_{11} + \alpha_{33}$, $\Delta\alpha = \alpha_{33} - \alpha_{11}$ and fluid bulk modulus K_f, in a fluid-saturated cracked rock of general TI symmetry. Those anisotropies are calculated from the combined use of the inverted low frequency compliances S_{ijkl}^{low} as given by (29) and relations (30). The low frequency predictions show that ε_{sat}^{low} and δ_{sat}^{low} have significantly lower values than their high frequency counterparts ε_{sat}^{high} and δ_{sat}^{high}, while γ_{sat}^{low} is close to γ_{sat}^{high}. If low frequency anisotropy is compared to its high frequency counterpart, a relatively smaller range of variation is observed for δ_{sat}^{low}, ε_{sat}^{low} and γ_{sat}^{low}. The implication is that laboratory data are **not** applicable directly to seismics and seismology, unless frequency corrections are performed. The assumption of ellipticity is approximately valid at low frequencies for a broad range of crack densities ($-0.2 \lesssim \Delta\alpha/\mathrm{tr}\,(\alpha_o) \lesssim 0.2$ and $\mathrm{tr}(\alpha)/\Delta\alpha_o \gtrsim 1$), for the set of parameters reported in Table 1.

Figure 4 compares the dry (plain curves) and saturated low frequency (dashed curves) predictions as a function of damage parameters $\mathrm{tr}(\alpha) = 2\ \alpha_{11} + \alpha_{33}$

and $\Delta\alpha = \alpha_{33} - \alpha_{11}$ in a cracked rock of general TI symmetry. We can note that: (i) ellipticity is observed both in the approximate dry and saturated (low frequency) cases, so that it is not a sufficient criterion to discriminate the underground saturation state; (ii) the strongest saturation effect (at low frequency) is observed on ε_{sat}^{low} and δ_{sat}^{low}. Therefore, those parameters may be used as a proxy for saturation; (iii) an opposite sign of the anellipticity parameter $\eta_{sat}^{low} \propto (\varepsilon_{sat}^{low} - \delta_{sat}^{low})$ characterizes the dry and saturated (low frequency), which may also useful as a proxy for saturation.

4 Conclusions

Elastic wave velocities and Thomsen's parameters have been calculated in cracked rocks. The background rock is assumed to be isotropic and the crack-induced anisotropy has been taken as that of transverse isotropy (TI).

Using effective medium theory (in the non-interaction approximation) and poroelasticity theory, high and low frequency elastic compliances have been calculated for both the fluid-saturated and dry cases. Thomsen's parameters have been also derived.

In the dry case, no frequency effect is predicted so that laboratory data are of direct applicability to seismics and seismology. In that case, approximate ellipticity is predicted. Crack densities can be inferred from Thomsen's parameters ε_{dry} ($\simeq \delta_{dry}$) and γ_{dry}.

In the saturated case, a strong frequency effect is predicted. Laboratory data are no longer directly applicable to seismics and seismology. Anellipticity is predicted at high frequency, but ellipticity is approximately valid at low frequency. Thomsen's parameters ε_{sat}^{low} and δ_{sat}^{low} may be used as a proxy for saturation discrimination. Crack densities may also be inferred from Thomsen's parameters ε_{sat}^{low} and γ_{sat}^{low}.

References

Benveniste, Y. (1987). A new approach to the application of the Mori-Tanaka's theory in composite materials. *Mech. Mater. 6*, 147–157.

Biot, M. A. (1941). General theory of three-dimensional consolidation. *J. Appl. Phys. 12*, 155–164.

Biot, M. A. (1956a). Theory of propagation of elastic waves in a fluid-saturated porous solid. I. Low-frequency range. *J. Acoust. Soc. Am. 28*(2), 168–178.

Biot, M. A. (1956b). Theory of propagation of elastic waves in a fluid-saturated porous solid. II. Higher frequency range. *J. Acoust. Soc. Am. 28*(2), 179–191.

Bristow, J. R. (1960). Microcracks and the static and dynamic elastic constants of annealed and heavily cold-worked metals. *Brit. J. Appl. Phys. 11*, 81–85.

Brown, R. and J. Korringa (1975). On the dependence of the elastic properties of a porous rock on the compressibitiy of the pore fluid. *Geophysics 40*(4), 608–616.

Bruner, W. M. (1976). Comment on "seismic velocities in dry and saturated cracked solids" by r. j. O'Connell and b. budiansky. *J. Geophys. Res. 81*, 2573–2578.

Budiansky, B. and R. J. O'Connell (1976). Elastic moduli of a cracked solid. *Int. J. Solids & Structures 12*, 81–97.

Gassman, F. (1951). über die elastizität poröser medien. *Vier. der Natur. Gesellschaft in Zürich 96*, 1–23.

Grechka, V. and M. Kachanov (2006). Effective elasticity of rocks with closely spaced and intersecting cracks. *Geophysics 71*, D85–D91.

Guéguen, Y., T. Chelidze, and M. L. Ravalec (1997). Microstructures, percolation thresholds, and rock physical properties. *Tectonophysics 279*, 23–35.

Guéguen, Y., L. Dormieux, and M. Boutéca (2004). *Fundamentals of Poromechanics*. Mechanics of Fluid-Saturated Rocks. Academic Press Elsevier.

Guéguen, Y. and V. Palciauskas (1994). *Introduction to the Physics of Rocks*. Princeton University Press.

Hashin, Z. (1983). Analysis of composite materials - a survey. *ASME J. Appl. Mech. 50*, 481–505.

Hill, R. (1965). A self-consistent mechanics of composite materials. *J. Mech. Phys. Solids 11*, 357–372.

Kachanov, M. (1992). Continuum model of medium with cracks. *ASCE J. Eng. Mech. 106*, 1039–1051.

Kachanov, M. (1993). Elastic solids with many cracks and related problems. *Adv. Appl. Mech. 30*, 259–445.

Kern, H. (1978). The effect of high temperature and high confining pressure on compressional wave velocities in quartz bearing and quartz free

igneous and metamorphic rocks. *Tetonophysics 44*, 185–203.

Le Ravalec, M. and Y. Guéguen (1996). High and low frequency elastic moduli for saturated porous/cracked rock: Differential self-consistent and poroelastic theories. *Geophysics 61*, 1080–1094.

Mori, S. and K. Tanaka (1973). Average stress in matrix and average elastic energy of materials with misfitting inclusions. *Acta Metall. 21*, 571–574.

Nye, J. F. (1979). *Physical Properties of Crystals*. Oxford University Press.

Saenger, E. H. (2007). Comment on "Comparison of the non-interaction and differential schemes in predicting the effective elastic properties of fractured media" by V. Grechka. *Int. J. Fracture*, 291–292.

Sarout, J. and Y. Guéguen (2008a). Anisotropy of elastic wave velocities in deformed shales-part i: Experimental results. *Geophysics*.

Sarout, J. and Y. Guéguen (2008b). Anisotropy of elastic wave velocities in deformed shales-part II: Modeling results. *Geophysics*.

Schubnel, A. and Y. Guéguen (2003). Dispersion and anisotropy of elastic waves in cracked rocks. *J. Geophys. Res. 108*.

Schubnel, A., O. Nishizawa, K. Masuda, X. J. Lei, Z. Xue, and Y. Guéguen (2003). Velocity measurements and crack density determination during wet triaxial experiments on oshima and toki granites. *Pure Appl. Geophys. 160*, 869–887.

Shafiro, B. and M. Kachanov (1997). Materials with fluid-filled pores of various shapes: Effective elastic properties and fluid pressure polarization. *Int. J. Solids & Structures 34*(27), 3517–3540.

Simmons, G. and W. F. Brace (1965). Comparison of static and dynamic measurements of compressibility of rocks. *J. Geophys. Res. 70*, 5649–5656.

Thomsen, L. (1986). Weak elastic anisotropy. *Geophysics 51*(10), 1954–1966.

Vavakin, A. S. and R. L. Salganik (1975). Effective characteristics of nonhomogeneous media with isolated inhomogeneities. *Mechanics of Solids, Allerton Press*, 58–66. English translation of Izvestia AN SSSR, Mekhanika Tverdogo Tela 10, 65-75.

Walsh, J. B. (1965). The effect of cracks on the compressibility of rocks. *J. Geophys. Res. 71*, 2591–2599.

Zimmerman, R. W. (1991). *Compressibility of Sandstones*. New York, USA: éd. Elsevier.

5 Figures

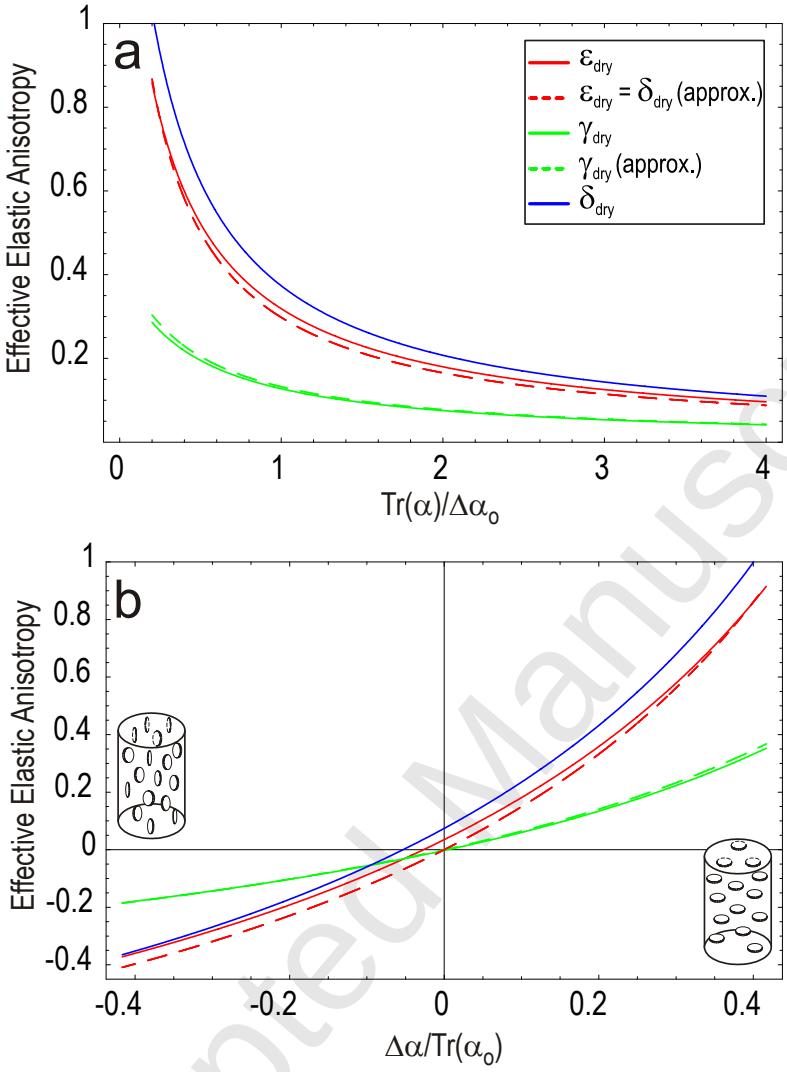

Fig. 1. Comparison of the actual (plain lines, β_{ijkl} not neglected) and the approximate (dashed lines, β_{ijkl} neglected) elastic anisotropies of a dry cracked rock.

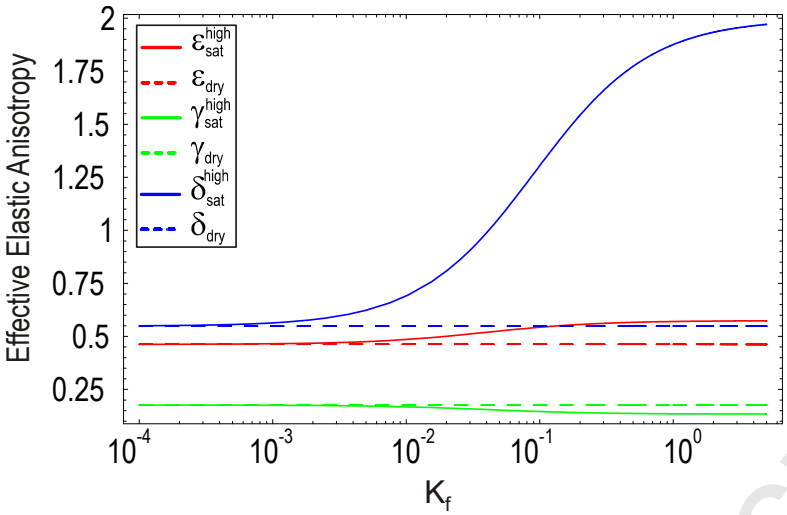

Fig. 2. Unrelaxed elastic anisotropy of a fluid-saturated cracked rock (plain lines for $K_f = 2.3$ GPa), and the corresponding dry anisotropy (dashed horizontal lines for $K_f = 0$). Also $\mathrm{tr}(\alpha) = \mathrm{tr}(\alpha_o)$ and $\Delta\alpha = \Delta\alpha_o$.

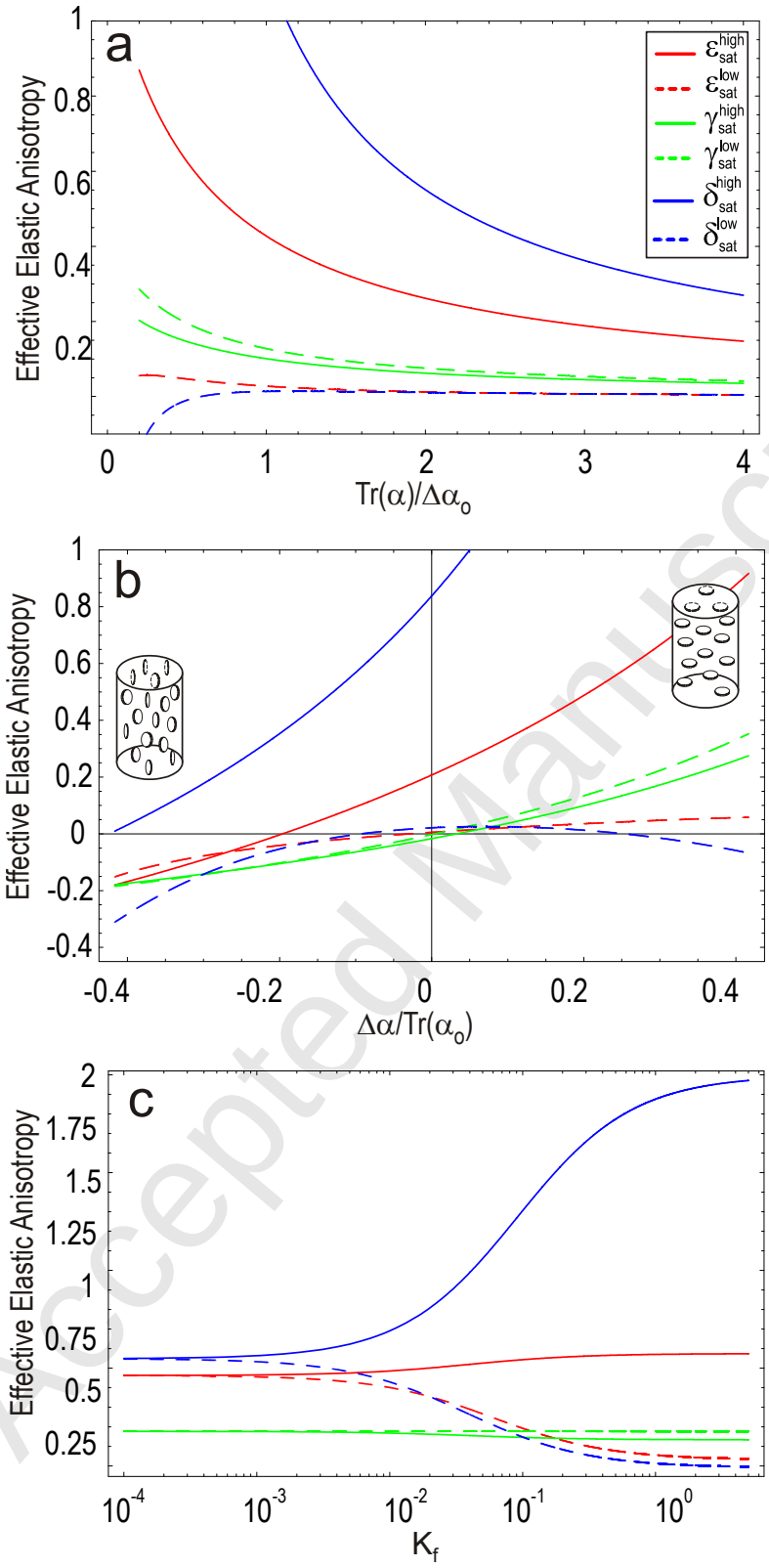

Fig. 3. Comparison of relaxed (low frequency, dashed lines) and unrelaxed (high frequency, plain lines) elastic anisotropies of a fluid-saturated cracked rock (for plot c, $\mathrm{tr}(\alpha) = \mathrm{tr}(\alpha_o)$ and $\Delta\alpha = \Delta\alpha_o$).

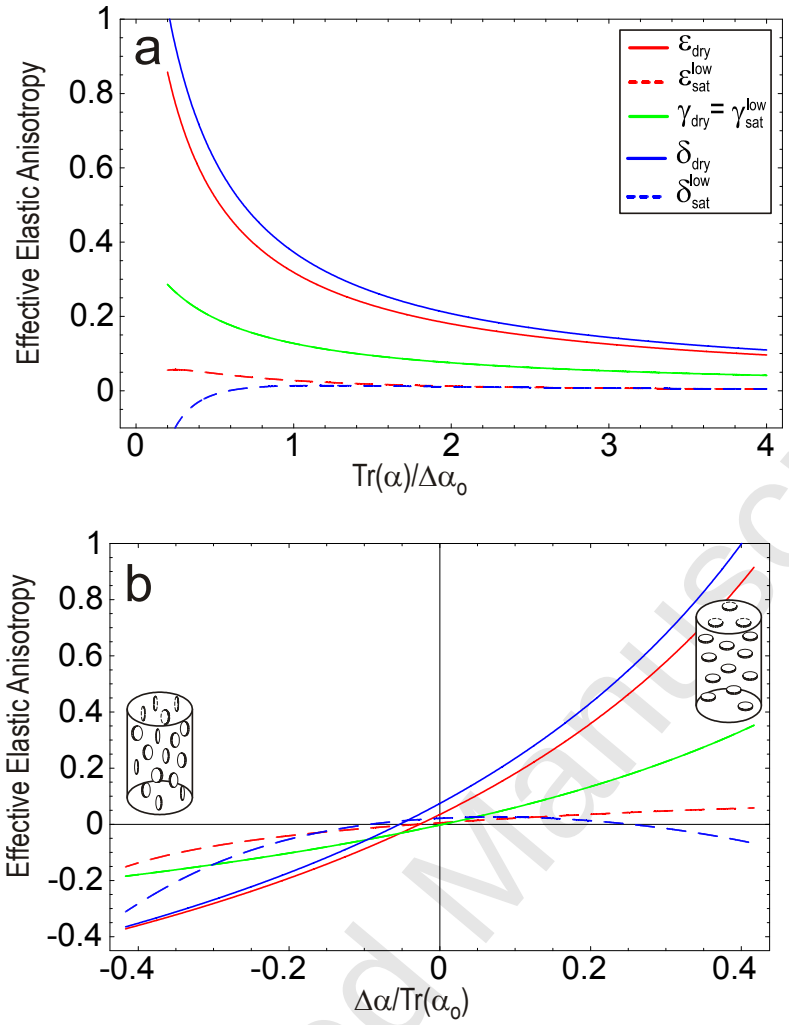

Fig. 4. Comparison of dry (plain lines) and relaxed (dashed lines) elastic anisotropies of a cracked rock.

6 Tables

Table 1
Range of damage parameters explored in the theoretical predictions for a dry cracked rock (crack porosity: 0.002).

	Ref. Value	**Range**	
$tr\,(\alpha) = 2\alpha_{11} + \alpha_{33}$	0.6	0.05	1
$\Delta\alpha = \alpha_{33} - \alpha_{11}$	0.25	-0.25	0.25
$\zeta = w/a$	$0.8{\times}10^{-3}$	$0.5{\times}10^{-3}$	$9.5{\times}10^{-3}$
β_{1111}	-0.1	*N/A*	
β_{1133}	-0.3	*N/A*	
β_{3333}	-0.025	*N/A*	